Genome analysis reveals hepatic transcriptional reprogramming changes mediated by enhancers during chick embryonic development

Xi Sun, Yumeng Wang, Chaohui Wang, Yibin Wang, Zhouzheng Ren, Xin Yang, Xiaojun Yang, and Yanli Liu [1]

College of Animal Science and Technology, Northwest A&F University, Yangling 712100, China

ABSTRACT The liver undergoes a slow process for lipid deposition during chick embryonic period. However, the underlying physiological and molecular mechanisms are still unclear. Therefore, the aim of the current study was to reveal the epigenetic mechanism of hepatic transcriptional reprogramming changes based on the integration analysis of RNA-seq and H3K27ac labeled CUT&Tag. Results showed that lipid contents increased gradually with the embryonic age (**E**) 11, E15, and E19 based on morphological analysis of Hematoxylin-eosin and Oil Red O staining as well as total triglyceride and cholesterol detection. The hepatic protein level of SREBP-1c was higher in E19 when compared with that in E11 and E15, while H3K27ac and H3K4me2 levels declined from E11 to E19. Differential expression genes (**DEGs**) among these 3 embryonic ages were determined by transcriptome analysis. A total of 107 and 46 genes were gradually upregulated and downregulated respectively with the embryonic age. Meanwhile, differential H3K27ac occupancy in chromatin was investigated. But the integration analysis of RNA-seq and CUT&Tag data showed that the overlap genes were less between DEGs and target genes of differential peaks in the promoter regions. Further, some KEGG pathways enriched from target genes of typical enhancer were overlapped with those from DEGs in transcriptome analysis such as insulin, FoxO, MAPK signaling pathways which were related to lipid metabolism. DNA motif analysis identify 8 and 10 transcription factors (**TFs**) based on up and down differential peaks individually among E11, E15, and E19 stages where 7 TFs were overlapped including COUP-TFII, FOXM1, FOXA1, HNF4A, RXR, ERRA, FOXA2. These results indicated that H3K27ac histone modification is involved in the transcriptional reprogramming regulation during embryonic development, which could recruit TFs binding to mediate differential enhancer activation. Differential activated enhancer impels dynamic transcriptional reprogramming towards lipid metabolism to promote the occurrence of special phenotype of hepatic lipid deposition.

Key words: chick embryo, hepatic transcriptome, transcription factors, H3K27 acetylation, enhancers

2023 Poultry Science 102:102516
https://doi.org/10.1016/j.psj.2023.102516

INTRODUCTION

The liver is one of the most important metabolic organs, governing many functions such as de novo lipogenesis (Leveille et al., 1975), detoxification (Zhao et al., 2019), hematopoietic (Robinson et al., 2016), and bile secretion (Goutam et al., 2022). It is a highly organized architecture that requires coordination by complex regulatory networks to maintain homeostasis. Liver dysfunction often leads to a variety of diseases in humans and animals, including non-alcohol fatty liver disease (**NAFLD**) (Kazankov et al., 2019), fatty liver hemorrhagic syndrome (**FLHS**) (Hamid et al. 2019), and cirrhosis (Singal and Mathurin, 2021). Hence, it is necessary to reveal the underlying regulatory mechanism of hepatic dynamic development.

Chick embryo has been widely used as the ideal model to explore the physiological and pathological research for the merits of easy manipulation and visualization (Vergara and Canto-Soler, 2012). On the other hand, the liver is the main site for lipid metabolism in chicks, but excessive abdominal fat deposition and FLHS caused enormous economic losses in poultry industry (Wang et al., 2017; Shini et al., 2019). All of these drive us to carry out the study to investigate hepatic embryonic development in chicks because the liver undergoes normal organ development and lipid deposition during embryonic period. Organ development is a systematic process along with transcriptional reprogramming (Hwang et al., 2018; Estermann et al., 2020) where great changes have taken place in chromatin accessibility and epigenetic

© 2023 The Authors. Published by Elsevier Inc. on behalf of Poultry Science Association Inc. This is an open access article under the CC BY-NC-ND license (http://creativecommons.org/licenses/by-nc-nd/4.0/).

Received October 17, 2022.
Accepted January 16, 2023.

[1]Corresponding author: liuyanli@nwsuaf.edu.cn

modifications (Kuznetsova et al., 2020). Many researchers have applied varies of methods to depict the hepatic metabolic or functional transitions during chick embryonic stages such as transcriptomics (Cogburn et al., 2018; Nguyen et al., 2022), proteomics (Yang et al., 2021a), and metabolomics (Liao et al., 2020), while few studies have focused on epigenetic changes.

Entanglement of DNA and histones in nucleus controlled the accessibility of transcription factors (**TFs**) and regulated gene expression. Histone modifications can serve as anchorage sites to recruit TFs and alter interacting nucleosomes. The histone H3 lysine 27 acetylation (**H3K27ac**) is positively correlated with transcription activation because it could shape a loosely chromatin state that allows TFs entry and promote the passage of RNA polymerase II (Valencia-Sánchez et al., 2021). Moreover, H3K27ac was considered as the marker of the promoter or enhancer regions, and both promoters and enhancers play important roles in transcriptional regulation process (Schoenfelder and Fraser, 2019; Chen et al., 2021). Thus, transcriptional regulation mechanism might be elucidated by integrating RNA-seq and histone modification analysis.

In the current study, we combined RNA-seq and H3K27ac-labeled CUT&Tag to evaluate developmental patterns in hepatic transcriptome and H3K27ac landscape of chick embryo, aiming to reveal the epigenetic mechanism of hepatic transcriptional reprogramming during chick embryonic period.

MATERIALS AND METHODS

All chick embryo and experimental protocol in the study were approved by the Institution Animal Care and Use Committee of the Northwest A&F University (Permit Number:DK202123).

Animals and Sample Collection

All hatching embryos were obtained from the Yangling Julong Poultry Industry Co. Ltd. (Yangling, China). At the embryonic day (**E**) 11, E15, and E19, some eggs with similar size and weight were taken out from the incubator for sampling collections. After cracking eggs and checking alive embryo, liver tissue was acquired by dissection. First, the blood contamination on the surface of the liver was washed away with ice-cold phosphate buffered saline; then filter paper was used to remove the liquid. Finally, about 1 cm^3 liver samples were clipped and fixed in 4% formaldehyde for histological analysis and other liver tissues were put into tubes for quick freeze of the liquid nitrogen. The frozen liver samples were transferred and stored at −80°C for subsequent analysis.

Hepatic Morphology

Fixed liver samples were processed in paraffin or frozen sections for hematoxylin-eosin (**HE**) and Oil Red O staining respectively, which was carried out by Wuhan Servicebio technology Co., Ltd (Wuhan, China).

Hepatic TG and TC Contents

About 50 mg liver tissue was cut from frozen liver and immediately homogenized in a high-throughput homogenizer with cold phosphate-buffered saline on the ice. The supernatant was collected after centrifugation at 3,000 rpm for 10 min at 4°C and the protein concentration of supernatant was determined by BCA Protein Assay Kit (Thermo Fisher Scientific, Shanghai, China). Meanwhile, the triglyceride (**TG**) and total cholesterol (**TC**) contents were detected using commercial kits according to the instructions of the kits and the data were converted by protein concentration correction.

Western Blotting

Small piece of frozen liver was cut and lysed with cold RIPA lysis buffer (ZhongHuiHeCai, Xi'an, China) with protease and phosphatase inhibitors on the ice. The BCA protein assay kits were used to determine the protein concentration of lysis supernatant. Then protein samples were denatured and performed for SDS-polyacrylamide gel electrophoresis separation to detect proteins expression. Detailed steps were reported to our previous study (Liu et al., 2018). The primary antibodies were used after 1:1,000 dilutions and their detailed information were as follows: β-actin (CWBIO, CW0096, Taizhou, China), SREBP (Wanleibio, wl01314, Shenyang, China), H3K27ac (Abcam, ab4729, MA), H3K4me2 (Abcam, ab32356, MA), and H3 (ABclonal, A2348, Wuhan, China). The secondary antibodies were used after 1:3,000 dilutions and goat anti-rabbit (No.122107) or mouse (No.117228) IgG HRP conjugated secondary antibody was bought from Jackson ImmunoResearch. The Image J software (National Institutes of Health, MD) was used to quantify blotting bands with β-actin or H3 as an internal control.

RNA-seq and RT-PCR

Total RNA was extracted from liver samples based on the introduction of TRIZOL reagent kits (TaKaRa, Dalian, China). RNA-seq libraries for each embryonic day were constructed by Shanghai Personal Biotechnology Co., Ltd and sequenced using Illumina NovaSeq. The sequencing reads data were firstly processed for checking the quality. The filtered reads were compared to the reference genome (GRCg7b, https://www.ncbi.nlm.nih.gov/genome/111) using HISAT2 software (http://ccb.jhu.edu/software/hisat2/index.shtml). The gene expression was normalized using Fragments Per Kilo bases per Million fragments (**FPKM**). Normalized read counts were used to identify differential expression genes (**DEGs**) by applying DESeq2 based on the parameters of log2 fold change > 1 and P-value < 0.05. The heat map packages were applied to map bivariate clustering for the comparison groups. All DEGs were annotated to the Database of Kyoto Encyclopedia of Genes and Genomes (**KEGG**, http://www.kegg.jp/); then KEGG enrichment analyses were carried out using

Clusterprofiler based on P-value <0.05. Detailed data processing for RNA-seq was referred to the previous report (Cogburn et al. 2018).

For RT-PCR, the extracted RNA was first converted into cDNA based on the protocol of UEIris RT mix with DNase (US Everbright Inc., Nanjing, China). Some DEGs were verified and evaluated their expression using 2 × SYBR Green qPCR Master Mix (US Everbright Inc.) on a Roche-LightCycler 96 instrument (Switzerland, Basel). Primer sequences are listed in Table 1. Detail PCR reaction and calculation methods are detailed in our previous study (Liu et al., 2020).

H3K27ac Labeled CUT-Tag Analysis

H3K27ac (Abcam, ab4729) labeled CUT-Tag assay was carried out to map chromatin epigenomic profiling based on the previous report (Kaya-Okur et al., 2019). Briefly, cell suspension was firstly prepared from liver samples. Concanavalin A-coated magnetic beads were added to mix with cells. Then H3K27ac primary antibody was incubated, followed by the secondary antibody. Next, Protein A-Tn5 adapter complex was added to the above system, which could recognize antibody. Finally, DNA was recovered from each sample after Tn5 transposase cuts the genome and inserts adapter sequences nearby the target protein. Library construction and sequencing were performed on an Illumina NovaSeq platform at Jiayin Biotechnology Ltd. (Shanghai, China). Clean reads were obtained and aligned to the reference chicken genome GRCg7b (https://www.ncbi.nlm.nih.gov/genome/111)) using BWA program. H3K27ac peaks were called by MACS2 and differential peaks were assessed using DESeq2 under the condition that the absolute value of the log2 fold change is >1 at a P-value <0.05. Heat map plots were drawn by the R based on the differentially peak analysis. Peaks were annotated by the function of annotatePeak of ChIPseeker and the promoter region was set as <3 kb from transcriptional start site where the target genes could also be predicted based on differential peaks in promoter regions.

Enhancer and DNA Motif Analysis

Based on the definition and identification method of super enhancer (**SE**) from Young lab (Whyte et al., 2013), ROSE software was employed to find super enhancer within 12.5 kb region of one another to be stitched together; all enhancers were firstly ranked, and the enhancers above the point of the slope 1 were regarded as SE while others as typical enhancer (**TE**). Targeted genes for enhancers were set within 100 kb distance to TSS from the peak center. The DNA sequence of differential peaks is compared with the Motif database (https://jaspar.genereg.net/) to perform DNA motif analysis based on HOMER tool.

Statistical Analysis

All experimental data were expressed as means and analyzed by one-way ANOVA using the GLM program of SPSS 20.0 (SPSS Inc., Chicago, IL). And Duncan's multiple comparisons test was used to determine significant differences among different embryonic days. A probability value less than 0.05 was considered statistically significant. Special statistical analysis for RNA-seq and CUT-Tag were mentioned and defined at the corresponding position when introducing methods above.

RESULTS

Phenotype Observation for Hepatic Lipid Metabolism of Chick Embryos

To investigate the dynamic changes of hepatic lipid metabolism during embryonic development in chicks, we performed HE and Oil Red O staining for the liver at E11, E15, and E19. As shown in Figure 1A, white

Table 1. Forward and reverse primer sequences for PCR analysis.

Gene	Accession number	Primer sequences, 5′ to 3′	Product size, bp
β-actin	L08165	F: ATTGTCCACCGCAAATGCTTC R: AAATAAAGCCATGCCAATCTCGTC	113
C21orf62	XM040658298	F: CTGTGACTACAGCCTGGCAA R:GTGCCACAGAAGGAGAGCTT	174
ITGBL1	XM046909491	F: GACGGAGGCTGGCAAATACT R: ACAGACCTTCCCGTCGTAGA	79
PDK4	NM001199909	F: CACCAAGGCCAAGGATGGAT R: ATGCACCAGTCATCTGCCTC	250
IGFBP2	NM001159982	F: TCACAACCACGAGGACTCAA R: AGCCATGCTTGTCACAGTTG	170
LBFABP	NM204634	F: CCAGGCAGACTGTGACTAACT R: CCATTTGCCAAGTGCACAGTA	100
CETP	NM001034814	F: AGTCTCGCCCTTCCTGAGAT R: GCAGCTTGGATAGTGACCGT	149
PCK1	NM205471	F: TCAACACCAGATTCCCAGGC R: CCTCATGCTAGCCACCACAT	137
FGF19	NM204674	F: TTCGTCCAGACGGCTACAAC R: CTCCACTGGCACAGTGTTGA	149
DNMT3b	NM001024828	F: CCCGTTATGATCGACGCTAT R: GGGCTACTCGCAGGCAAA	225

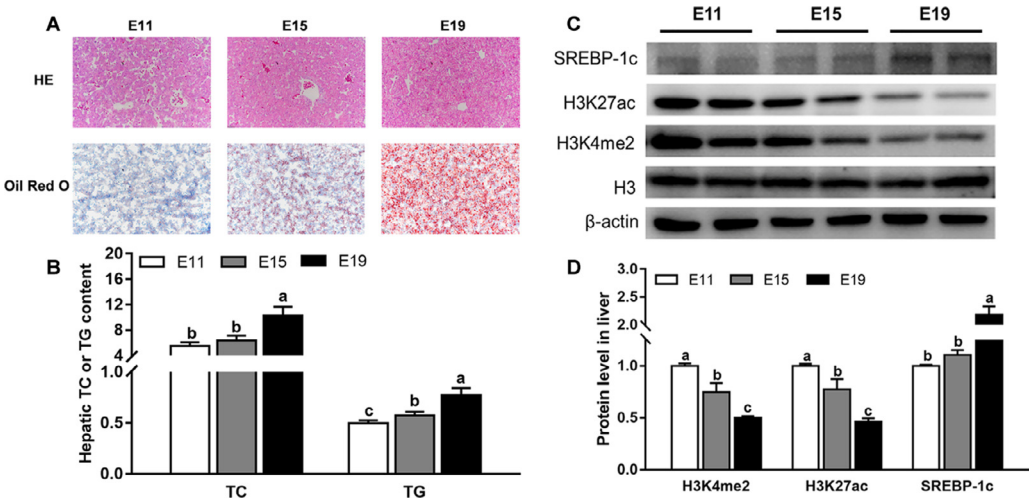

Figure 1. Phenotype observation for hepatic lipid metabolism of chick embryos. (A) Histological sections stained by H&E and Oil Red O (magnification:10 × 20), respectively. (B) TG and TC contents in the liver. (C) Western blot analysis for protein molecules about histone modification and lipogenesis. (D) The quantification of western blot bands where SREBP-1c was normalized to β-actin and histone modification was normalized to H3. All data are expressed as mean ± SEM (n = 6). $^{a-c}$Values with different superscript letters on the bars are statistical significant ($P < 0.05$). Abbreviations: TC, total cholesterol; TG, triglyceride.

cavities and red lipid droplets became more and more with the increasing of embryonic day. The contents of hepatic total TG and TC were found to be higher at E19 when compared with those at E11 and E15 (Figure 1B). In addition, the protein expression of SREBP-1c, which is related to lipogenesis, was also higher at E19 (Figures 1C and 1D). Simultaneously, hepatic H3K4me2 and H3K27ac protein abundance, markers of transcriptional activation, decreased gradually along with the embryonic development (Figures 1Cand 1D).

DEGs Identification and KEGG Pathway Enriched From Transcriptome Analysis

To reveal hepatic transcriptional reprogramming during chick embryonic development, transcriptome was applied to detect DEGs. As shown in Figure 2A, the number of upregulated and downregulated DEGs between E11 and E15 was 358 and 174 respectively. While the number of DEGs between E15 and E19 was 689 upregulation and 800 downregulation. The heatmap for cluster analysis of DEGs showed that some genes were increased or decreased gradually with embryonic days (Figure 2B). The number of up- and downregulation genes among E11 vs. E15 vs. E19 comparison was 106 and 47 separately (Figures 2C and 2D). We selected 9 genes that are interrelated to hepatic development or lipid metabolism to verify their mRNA abundance by RT-PCR. As demonstrated in Figures 2E−2M, C21orf62, ITGBL1, PDK4, IGFBP2, LBFABP, and CETP were elevated constantly, while PCK1, FGF19 and DMNT3b were decreased sharply with embryonic development, which were consistent with RNA-seq results.

For a better understanding of DEGs, we further performed KEGG enrichment analysis to predict the potential metabolic pathway during embryonic development. As shown in Figures S1 and S2, total, up and down DEGs were used for KEGG pathway analysis, respectively. Metabolic pathways related to liver organ development were significantly enriched such as cell adhesion, cell cycle, DNA replication. Especially, insulin and FoxO signaling pathways, involving in lipogenesis, were gathered based on up DEGs from E15 vs. E19 and E11 vs. E15 vs. E19 (Figures S1E and S2B).

Differential H3K27ac Regions and Targeted Genes Based on CUT&Tag Analysis

To address whether H3K27ac, a histone modification of active promoters and enhancers, was involved in the regulation of transcriptional reprogramming, we examined the genome-wide H3K27ac profiling in the liver of chick embryo. As shown in Figure 3, when compared with E11, 1,148 hyperacetylated and 2,422 hypoacetylated peaks were obtained at E15. Similarly, a total of 7,032 differential H3K27ac regions were observed at E19 in comparison with those at E15. Ulteriorly, poorly, or highly differential acetylated peaks in the promoter region were selected for predicting down- or upregulated target genes, which were used to overlap with DEGs identified from transcriptome analysis. However, only 12 upregulation and 8 downregulation genes were linked between E11 and E15 (Figures 4A and 4B), which accounted for just 4% of all DEGs; likewise, overlapped genes between E15 and E19 occupied 11% among more than 1,400 DGEs (Figures 4C and 4D). In order to reveal whether enhancers are involved in hepatic transcriptional reprogramming, differential typical and super enhancers were distinguished. As demonstrated in Figures 4E and 4F, a total of 781 (E15 vs. E11) and 1,086 (E19 vs. E15) typical enhancers were found, respectively.

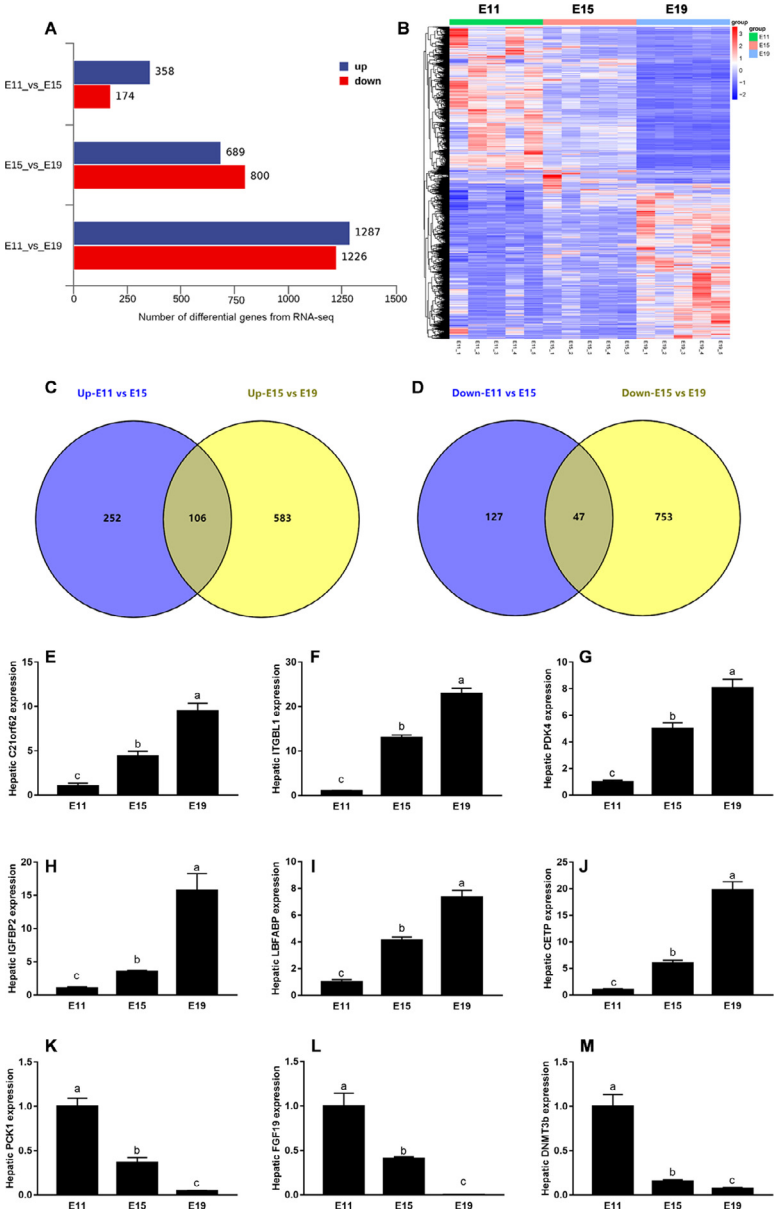

Figure 2. DEGs identification during embryonic development based on transcriptome analysis. (A) The number of DEGs in pairwise comparison among three embryonic days. (B) The heat map of hepatic DEGs. Higher expression genes were shown in red color, whereas lower genes are presented in blue color. (C, D) Venn diagram for overlapping up and down DEGs between E11 vs. E15 and E15 vs. E19. (E–M) Genes expression of selected DEGs by RT-PCR. Data are expressed as mean ± SEM (n = 5). $^{a-c}$Values with different superscript letters on the bars are statistical significant ($P < 0.05$). Abbreviation: DEGs, differential expression genes.

KEGG Pathway Enriched From Differential Enhancers-Predicted Genes

Considering the enhancer function on gene transcription via enhancer-promoter loop, we then performed KEGG pathway enrichment analysis based on predicted target genes from up- or downregulation enhancers. As presented in Figure 5, metabolic pathways about liver organ development were observed on basis of upregulation enhancer-predicted genes such as tight junction, cell cycle, and VEGF signaling between E15 and E11 comparison as well as focal adhesion in the E19 vs. E15 comparison; lipid metabolism pathways including glycerolipid metabolism, insulin, FoxO, and MAPK signaling were also significantly enriched along with embryonic day. These pathways based on enhancers-predicted gene lists were shared with KEGG pathways enriched from DEGs of RNA-seq analysis.

DNA Motifs Prediction Based on Differential H3K27ac Peaks

TFs and coactivators or chromatin remodeling complexes are required for enhancers to interact proximity with their target promoters in 3D space. The top 20 DNA motifs were shown in Figures 6A–6D based on up or down differential peaks for E11 vs. E15 and E15 vs. E19 severally. We performed the intersection analysis and found that there were 8 and 10 TF binding motifs

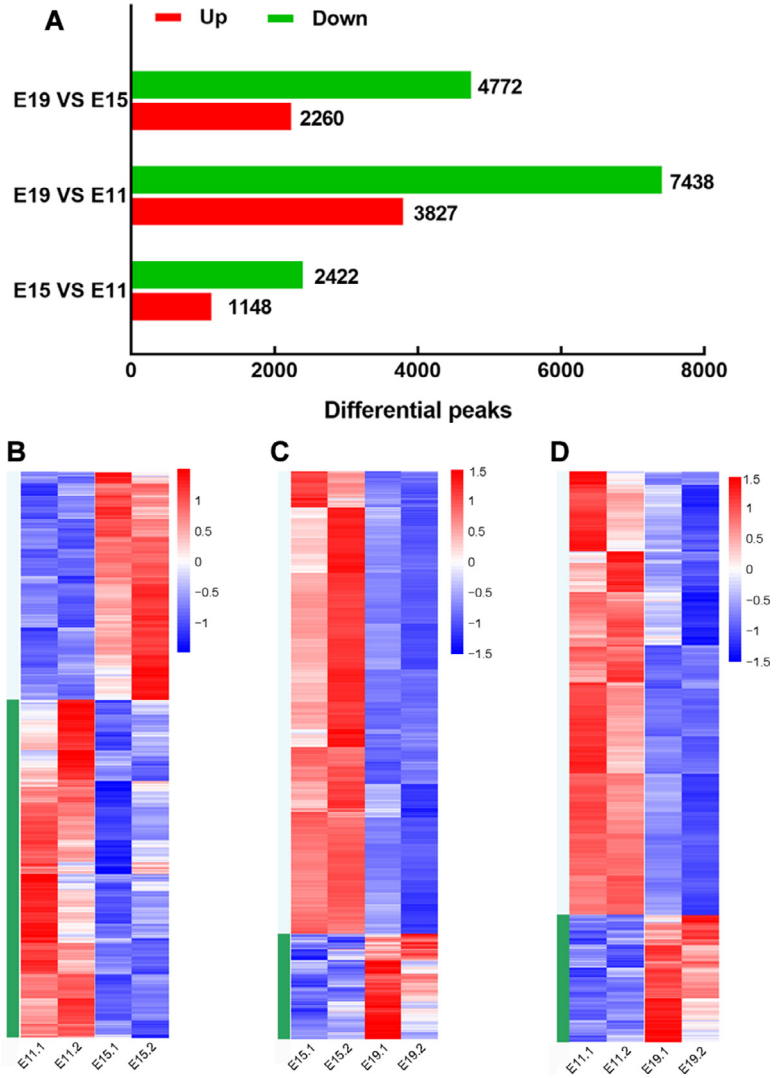

Figure 3. Differential peaks analysis through H3K27ac labeled CUT&Tag (n = 2). (A) The number of differentially acetylated peaks in pairwise comparison among three embryonic days. (B–D) The heat map of differentially acetylated peaks in the liver. The upregulated peaks are shown in red color, whereas the downregulated peaks are presented in blue color.

enriched by up or down differential H3K27ac peaks respectively along with embryonic days (Figures 6E and 6F). Among these TF binding motifs from different trend peaks, 7 TFs are the same including COUP-TFII, FOXM1, FOXA1, HNF4A, RXR, ERRA, and FOXA2.

DISCUSSION

The chick embryo is an easily operating and accessible model, whose physiological and pathological changes can be detected and visualized straightforwardly, thus it is usually employed for immune research (Garcia et al., 2021), drug evaluation (Wu et al., 2018b), cancer (Ribatti and Tamma, 2018), and epigenetic research (Bednarczyk et al., 2021). As a multifunctional organ, liver is involved in detoxification, bile secretion, and is also the main organ of de novo lipogenesis in humans and chicks. When dysregulated, the hepatic homeostasis was disturbed and many diseases followed. In our previous study, we analyzed morphological characteristics in the liver of chicks and found that hepatic lipids increased gradually during embryonic period (Liu et al., 2020), and the same results were found in the current study that lipid contents were increased along with the embryonic day. In addition, hepatic abundance of adipogenic marker SREBP-1c progressively increased in protein level, suggesting that hepatic lipid metabolism has experienced significant changes.

Previous study reported that great changes genome-wide H3K27ac profiles changed a lot in the liver of FLHS chicks (Zhu et al., 2020). Consistent with the results in the present study, hepatic total H3K27ac and H3K4me2 levels were different among 3 embryonic days. These 2 epigenetic modifications were considered to be the marker for identifying enhancers and promoters (Hnisz et al., 2013) and positively associated with genes expression (Zheng et al., 2019). These results suggested that transcriptional reprogramming of hepatic lipid metabolism has changed along with chick embryonic development, which might be mediated by histone epigenetic modifications.

To uncover hepatic transcriptional changes, we applied RNA-seq to detect gene expression patterns

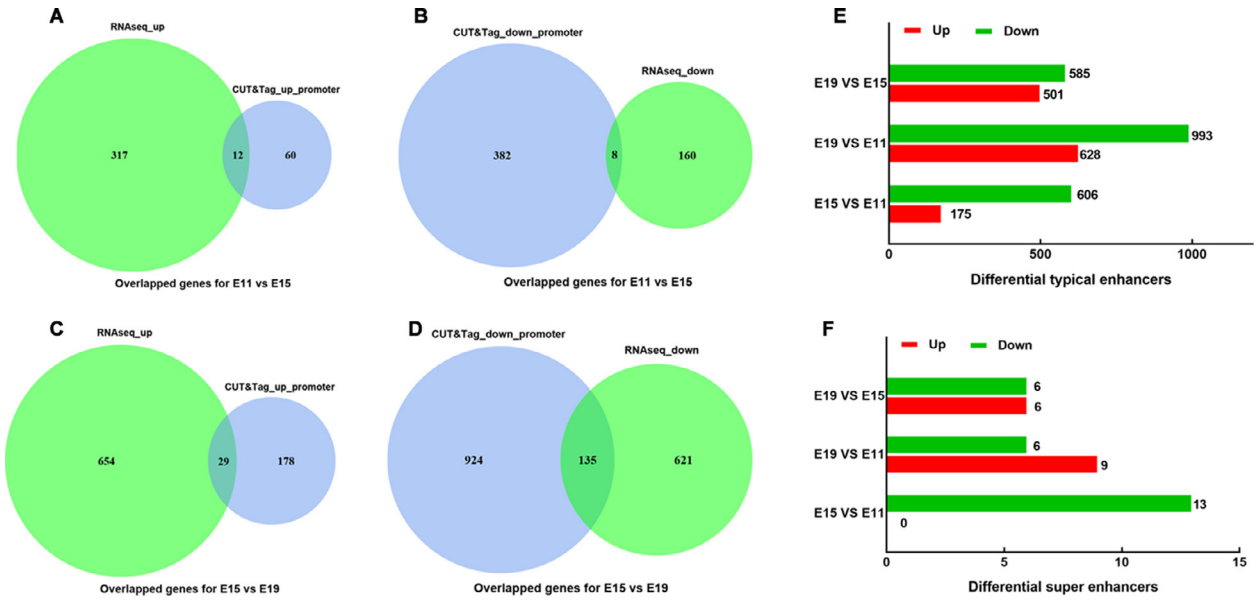

Figure 4. Overlap genes analysis and enhancer identification. (A−D) Venn diagram for overlap genes obtained from DEGs and target genes of differential peaks in the promoter. Up DEGs were overlapped with target genes of hyperacetylated differential peaks in the promoter while down DEGs with hypoacetylated differential peaks. (E) The number of differential typical enhancers in pairwise comparison among three embryonic days. (F) The number of differential super enhancers in pairwise comparison among three embryonic days. Abbreviation: DEGs, differential expression genes.

during E11, E15, and E19. Results showed that some genes were increased or decreased gradually with embryonic days. Among DEGs from E11 vs. E15 vs. E19 comparison, we selected 9 genes which were involved in hepatic development or lipid metabolism for subsequent RT-PCR verification. ITGBL1 is considered as the hub gene interrelated to hepatic fibrogenesis, cell migration, and adhesion (Li et al., 2015; Huang et al., 2020). FGF19, as a member of fibroblast growth factors, was closely related to embryonic development. PDK4 is a critical regulator of lipid metabolism and could coordinate with liver growth (Zhao et al., 2020) as well as hepatocyte apoptosis (Wu et al., 2018a). IGFBP2, LBFABP, and CETP were involved in hepatic energy or lipid metabolism. In the present study, these genes expression increased during embryonic development, which was in accordance with the phenotype of hepatic lipid deposition. Indeed, KEGG pathway analysis showed that cell adhesion, insulin, and FoxO signaling pathways were enriched based on up DEGs which were related to organ development or lipogenesis. In contrary, some pathways associated with lipid catabolism were gained from down DEGs such as MAPK signaling, fatty acid degradation and so on. PCK1 is decreased dramatically with embryonic development, which acts as the rate-limiting enzyme in gluconeogenesis. Previous study has shown that glycolysis is not the main way to generate energy from E19 to hatching in chicks (Hu et al., 2017). Collectively, these results demonstrated that hepatic transcriptional change was toward lipid deposition with chick embryonic growth. However, genetic and molecular mechanisms underlying transcriptional reprogramming remain largely unknown.

Considering the role of H3K27ac in gene transcription (Dunislawska et al., 2022) and its dynamic changes along with chick embryonic growth in the study, we speculated that H3K27ac epigenetic modification might take part in hepatic transcriptional reprogramming. We then applied H3K27ac labeled Cut-Tag assays to assess genome-wide H3K27ac profiling in the liver. As we all known, gene transcription is strictly controlled by promoters and H3K27ac is a feature of accessible chromatin. Thus, differential H3K27ac peaks in the promoter regions were firstly used to predict target genes. But unexpectedly, the overlap genes were less when linked with transcriptome-identified DEGs, indicating that our traditional understanding might be biased. Except for promoters, enhancers also take part in the regulation of gene expression as the regulatory element (Marsman and Horsfield, 2012; Zabidi and Stark, 2016; Andersson and Sandelin, 2020), which recruit TFs and cofactors to activate transcription from target promoters via enhancer-promoter loop 3D structure (Sengupta and George, 2017). Then differential enhancers were identified and used for differential genes prediction, while numbers of enhances and predicted genes were far more than DEGs obtained from transcriptomics. Overlap analysis might be not suitable for linking predicted or differential genes from 2 methods. Hence, we mapped predicted genes from differential enhancer to KEGG database to monitor potential metabolic pathway changes. Surprisingly, focal adhesions, tight junction, cell cycle, insulin and FoxO signaling, glycerolipid metabolism, fatty acid elongation pathways were significantly enriched based on predicted genes from upregulation enhancers. These pathways are consistent with those obtained from DEGs in the study. During chick embryonic period, the liver organ is still undergoing growth development.

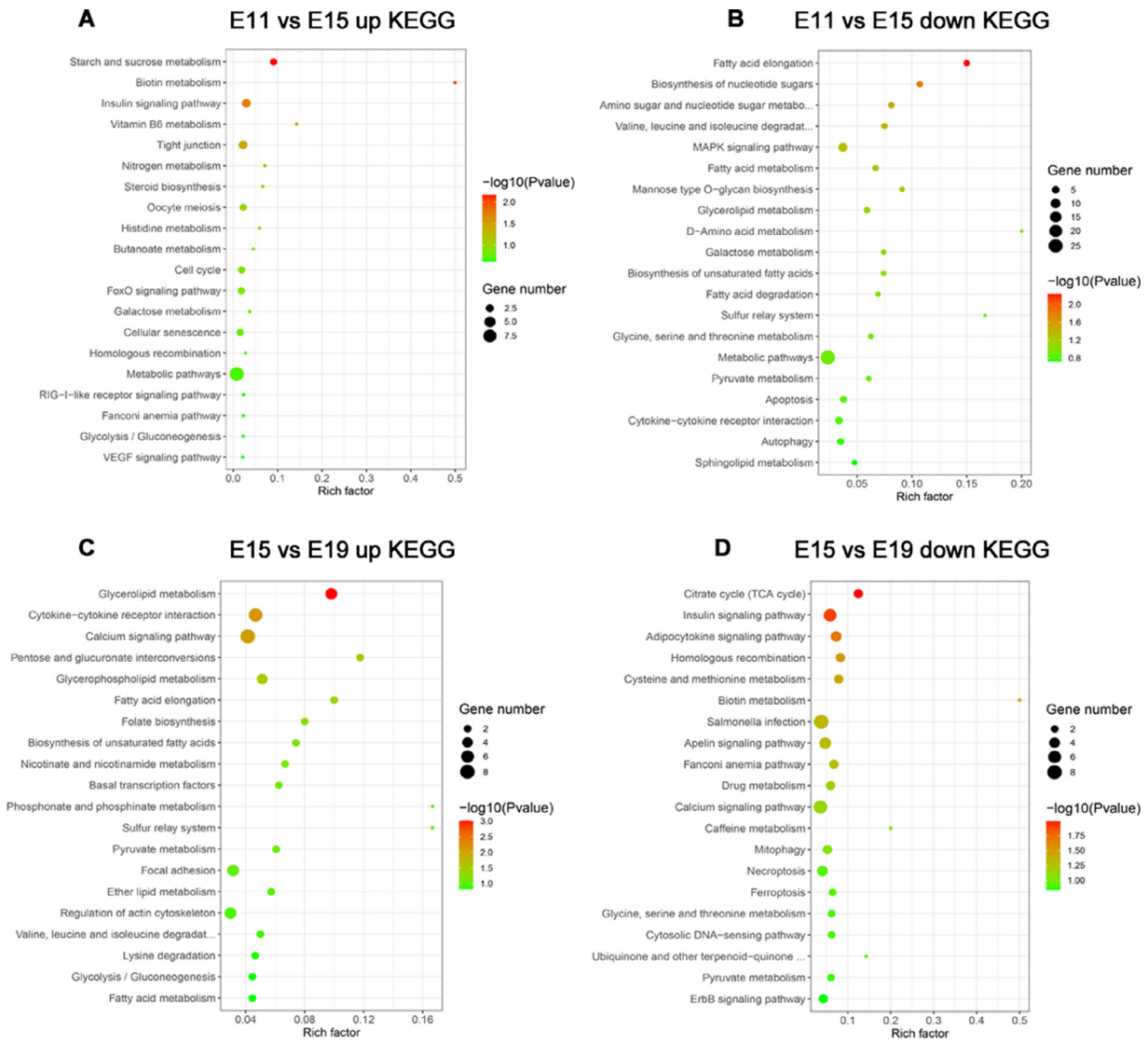

Figure 5. KEGG analysis based on the differential typical enhancers-predicted genes. Target genes predicted from up differential typical enhancers were used for up KEGG pathways enrichment (A and C). Likewise, down KEGG pathways were enriched from target genes of down differential enhancer (B and D). The larger size circles indicated more genes contributing to the enriched pathway, and the color indicated pathway impact values from green to red.

Focal adhesion and tight junction-related pathways help maintain cell proliferation and differentiation in the process of liver structure formation (Singh et al., 2017; Du et al., 2021). All these findings suggested that the enhancer was potentially participated in regulating hepatic transcriptional reprogramming.

It is reported that TFs contribute to enhancers-mediated gene transcription via promoting enhancer-promoter loop formation (Weintraub et al., 2017). We next sought to interrogate the potential TFs involved in enhancers-mediated 3D chromatin structure. DNA motif analysis based on up or down differential peaks identified 7 TFs that are shared including COUP-TFII, FOXM1, FOXA1, HNF4A, RXR, ERRA, and FOXA2. COUP-TFII has been shown to be involved in the regulation of metabolic processes, such as adipogenic, gluconeogenesis, and cholesterol processing in the liver (Ashraf et al., 2019). As a pioneer TF, FOXA1 cell type-specific functions mainly depended on differential recruitment to chromatin at distant enhancers rather than promoters (Lupien et al., 2008). FOXM1 is a typical proliferation-related transcription factor, which regulates cell proliferation through a cell cycle-dependent manner (Wang et al., 2001; Hu et al., 2019). Many reports support the notion that HNF4A is a master regulator of hepatocyte phenotype and can regulate gene expression by binding promoter regions and coordinating lipolysis, p53, and bile acid signaling pathways, thereby preventing diet-induced NAFLD development (Xu et al., 2021; Yang et al., 2021b). RXR, ERRA and FOXA2 were reported to develop functions in lipid metabolism, endocrine, and immune system, respectively (Wahab et al., 2019; Helmstädter et al., 2022; Yánez et al., 2022). Taken together, these screened TFs might be involved in the regulation of organ development and lipid metabolism during embryonic periods. But 7 TFs mentioned above were screened from both up and down differential peaks, implying that TFs could dynamically bind various DNA positions to mediate epigenetic regulation.

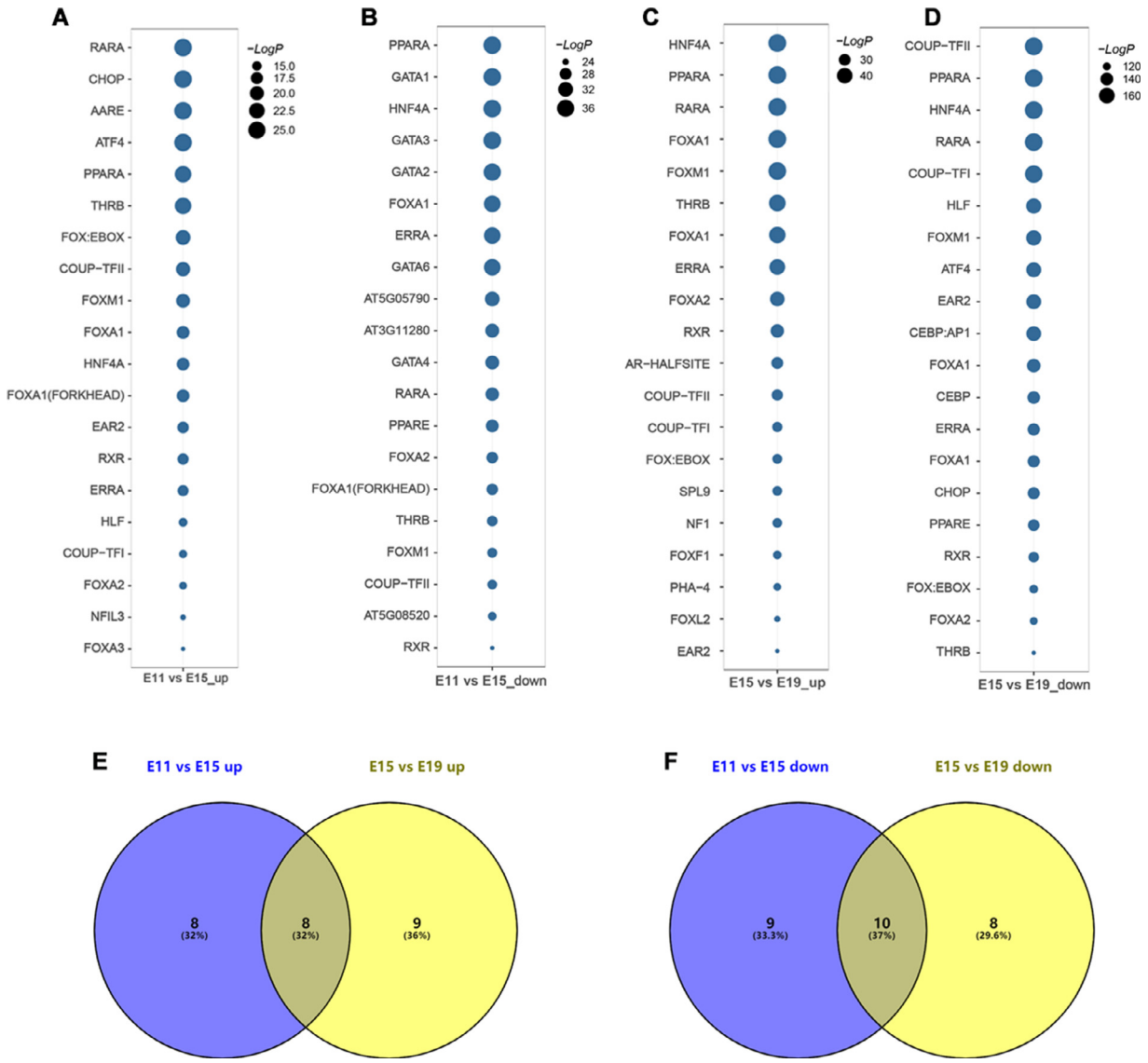

Figure 6. DNA motifs analysis based on differential H3K27ac peaks. (A, B) DNA motifs predicted from up and down differential H3K27ac peaks for E11 vs. E15, respectively. (C, D) DNA motifs predicted from up and down differential H3K27ac peaks for E15 vs. E19, respectively.

CONCLUSIONS

In summary, our results found H3K27ac histone modifications could mediate enhancer activation by recruiting TFs binding, leading to hepatic transcriptional reprogramming toward organ development and lipid metabolism during embryonic stages. These observations expand current knowledge and provide new insights into transcriptional regulation of liver organ development of chick embryo.

ACKNOWLEDGMENTS

This work was funded by the National Science Foundation of China (32102567), the Program for Shaanxi Science & Technology (2023-YBNY-144, 2022KJXX-13, 2019ZDXM3-02 and 2021TD-30), Chinese Universities Scientific Fund (2452021002), Innovation and entrepreneurship training program for college students (202110712048).

Authors' contribution: YLL designed the research; XS, YMW, CHW and YBW performed the research and analyzed the data; XS, YM and YLL wrote the manuscript; YLD, XY and XJY have taken part in the revision of the manuscript. The author confirmed that all data underlying the findings in the current study are fully available without restriction from the corresponding author on reasonable request.

DISCLOSURES

The authors declare that they have no competing interests.

SUPPLEMENTARY MATERIALS

Supplementary material associated with this article can be found in the online version at doi:10.1016/j.psj.2023.102516.

REFERENCES

Andersson, R., and A. Sandelin. 2020. Determinants of enhancer and promoter activities of regulatory elements. Nat. Rev. Genet. 21:71–87.

Ashraf, U. M., E. R. Sanchez, and S. Kumarasamy. 2019. COUP-TFII revisited: its role in metabolic gene regulation. Steroids 141:63–69.

Bednarczyk, M., A. Dunislawska, K. Stadnicka, and E. Grochowska. 2021. Chicken embryo as a model in epigenetic research. Poult. Sci. 100:101164–101176.

Chen, L., W. Cao, R. Aita, D. Aldea, J. Flores, N. Gao, E. M. Bonder, C. E. Ellison, and M. P. Verzi. 2021. Three-dimensional interactions between enhancers and promoters during intestinal differentiation depend upon HNF4. Cell Rep 34:108679–108707.

Cogburn, L. A., N. Trakooljul, C. Chen, H. Huang, C. H. Wu, W. Carré, X. Wang, and H. B. White 3rd. 2018. Transcriptional profiling of liver during the critical embryo-to-hatchling transition period in the chicken (Gallus gallus). BMC Genomics 19:695–732.

Du, H., X. Yang, J. Fan, and X. Du. 2021. Claudin 6: Therapeutic prospects for tumours, and mechanisms of expression and regulation (Review). Mol. Med. Rep. 24:667–676.

Dunislawska, A., E. Pietrzak, R. Wishna Kadawarage, A. Beldowska, and M. Siwek. 2022. Pre-hatching and post-hatching environmental factors related to epigenetic mechanisms in poultry. J Anim. Sci. 100:370–382.

Estermann, M. A., S. Williams, C. E. Hirst, Z. Y. Roly, O. Serralbo, D. Adhikari, D. Powell, A. T. Major, and C. A. Smith. 2020. Insights into gonadal sex differentiation provided by single-cell transcriptomics in the chicken embryo. Cell Rep 31:107491–107516.

Garcia, P., Y. Wang, J. Viallet, and Z. Macek Jilkova. 2021. The chicken embryo model: a novel and relevant model for immune-based studies. Front. Immunol. 12:791081–791097.

Goutam, K., F. S. Ielasi, E. Pardon, J. Steyaert, and N. Reyes. 2022. Structural basis of sodium-dependent bile salt uptake into the liver. Nature 606:1015–1020.

Hamid, H., J. Y. Zhang, W. X. Li, C. Liu, M. L. Li, L. H. Zhao, C. Ji, and Q. G. Ma. 2019. Interactions between the cecal microbiota and non-alcoholic steatohepatitis using laying hens as the model. Poult. Sci. 98:2509–2521.

Helmstädter, M., S. Schierle, L. Isigkeit, E. Proschak, J. A. Marschner, and D. Merk. 2022. Activity screening of fatty acid mimetic drugs identified nuclear receptor agonists. Int. J. Mol. Sci 23:10070–10082.

Hnisz, D., B. J. Abraham, T. I. Lee, A. Lau, V. Saint-André, A. A. Sigova, H. A. Hoke, and R. A. Young. 2013. Super-enhancers in the control of cell identity and disease. Cell 155:934–947.

Hu, Q., U. Agarwal, and B. J. Bequette. 2017. Gluconeogenesis, non-essential amino acid synthesis and substrate partitioning in chicken embryos during later development. Poult. Sci. 96:414–424.

Hu, G., Z. Yan, C. Zhang, M. Cheng, Y. Yan, Y. Wang, L. Deng, Q. Lu, and S. Luo. 2019. FOXM1 promotes hepatocellular carcinoma progression by regulating KIF4A expression. J. Exp. Clin. Cancer Res. 38:188–205.

Huang, W., D. Yu, M. Wang, Y. Han, J. Lin, D. Wei, J. Cai, B. Li, P. Chen, and X. Zhang. 2020. ITGBL1 promotes cell migration and invasion through stimulating the TGF-β signalling pathway in hepatocellular carcinoma. Cell Prolif 53:12836–12852.

Hwang, Y. S., M. Seo, S. Bang, H. Kim, and J. Y. Han. 2018. Transcriptional and translational dynamics during maternal-to-zygotic transition in early chicken development. FASEB J. 32:2004–2011.

Kaya-Okur, H. S., S. J. Wu, C. A. Codomo, E. S. Pledger, and S. Henikoff. 2019. CUT&Tag for efficient epigenomic profiling of small samples and single cells. Nat. Commun. 10:1930–1940.

Kazankov, K., S. M. D. Jørgensen, K. L. Thomsen, H. J. Møller, H. Vilstrup, J. George, D. Schuppan, and H. Grønbæk. 2019. The role of macrophages in nonalcoholic fatty liver disease and nonalcoholic steatohepatitis. Nat. Rev. Gastroenterol. Hepatol. 16:145–159.

Kuznetsova, T., K. H. M. Prange, C. K. Glass, and M. P. J. de Winther. 2020. Transcriptional and epigenetic regulation of macrophages in atherosclerosis. Nat. Rev. Cardiol. 17:216–228.

Leveille, G. A., D. R. Romsos, Y. Yeh, and E. K. O'Hea. 1975. Lipid biosynthesis in the chick. A consideration of site of synthesis, influence of diet and possible regulatory mechanisms. Poult. Sci. 54:1075–1093.

Li, X. Q., X. Du, D. M. Li, P. Z. Kong, Y. Sun, P. F. Liu, Q. S. Wang, and Y. M. Feng. 2015. ITGBL1 is a runx2 transcriptional target and promotes breast cancer bone metastasis by activating the TGFβ signaling pathway. Cancer Res 75:3302–3313.

Liao, G., X. Song, X. Wang, W. Zhang, L. Zhang, J. Qiu, and R. Hou. 2020. Cytotoxicity of 2,2′,3,5′,6-Pentachlorobiphenyl (PCB95) and its metabolites in the chicken embryo liver cells of laying hens. Ecotoxicol. Environ. Saf. 194:110338–110347.

Liu, Y., J. Shen, X. Yang, Q. Sun, and X. Yang. 2018. Folic acid reduced triglycerides deposition in primary chicken hepatocytes. J. Agric. Food. Chem. 66:13162–13172.

Liu, Y., J. Zhou, B. B. Musa, H. Khawar, X. Yang, Y. Cao, and X. Yang. 2020. Developmental changes in hepatic lipid metabolism of chicks during the embryonic periods and the first week of post-hatch. Poult. Sci. 99:1655–1662.

Lupien, M., J. Eeckhoute, C. A. Meyer, Q. Wang, Y. Zhang, W. Li, J. S. Carroll, X. S. Liu, and M. Brown. 2008. FoxA1 translates epigenetic signatures into enhancer-driven lineage-specific transcription. Cell 132:958–970.

Marsman, J., and J. A. Horsfield. 2012. Long distance relationships: enhancer-promoter communication and dynamic gene transcription. Biochim. Biophys. Acta. 1819:1217–1227.

Nguyen, P. T. T., F. Pagé-Larivière, K. Williams, J. O'Brien, and D. Crump. 2022. Developmental and hepatic gene expression changes in chicken embryos exposed to p-Tert-Butylphenyl diphenyl phosphate and isopropylphenyl phosphate via egg injection. Environ. Toxicol. Chem. 41:739–747.

Ribatti, D., and R. Tamma. 2018. The chick embryo chorioallantoic membrane as an in vivo experimental model to study human neuroblastoma. J. Cell. Physiol. 234:152–157.

Robinson, M. W., C. Harmon, and C. O'Farrelly. 2016. Liver immunology and its role in inflammation and homeostasis. Cell Mol. Immunol. 13:267–276.

Schoenfelder, S., and P. Fraser. 2019. Long-range enhancer-promoter contacts in gene expression control. Nat. Rev. Genet. 20:437–455.

Sengupta, S., and R. E. George. 2017. Super-enhancer-driven transcriptional dependencies in cancer. Trends Cancer 3:269–281.

Shini, A., S. Shini, and W. L. Bryden. 2019. Fatty liver haemorrhagic syndrome occurrence in laying hens: impact of production system. Avian Pathol 48:25–34.

Singal, A. K., and P. Mathurin. 2021. Diagnosis and treatment of alcohol-associated liver disease: a review. JAMA 326:165–176.

Singh, A. B., S. B. Uppada, and P. Dhawan. 2017. Claudin proteins, outside-in signaling, and carcinogenesis. Pflugers. Arch. 469:69–75.

Valencia-Sánchez, M. I., P. De Ioannes, M. Wang, D. M. Truong, R. Lee, J. P. Armache, J. D. Boeke, and K. J. Armache. 2021. Regulation of the Dot1 histone H3K79 methyltransferase by histone H4K16 acetylation. Science 371:6663–6688.

Vergara, M. N., and M. V. Canto-Soler. 2012. Rediscovering the chick embryo as a model to study retinal development. Neural. Nev. 7:22–41.

Wahab, F., I. U. Khan, I. R. Polo, H. Zubair, C. Drummer, M. Shahab, and R. Behr. 2019. Irisin in the primate hypothalamus and its effect on GnRH in vitro. J. Endocrinol. 241:175–187.

Wang, G., W. K. Kim, M. A. Cline, and E. R. Gilbert. 2017. Factors affecting adipose tissue development in chickens: a review. Poult. Sci. 96:3687–3699.

Wang, X., E. Quail, N. J. Hung, Y. Tan, H. Ye, and R. H. Costa. 2001. Increased levels of forkhead box M1B transcription factor in transgenic mouse hepatocytes prevent age-related proliferation defects in regenerating liver. Proc. Natl. Acad. Sci. U. S. A. 98:11468–11473.

Weintraub, A. S., C. H. Li, A. V. Zamudio, A. A. Sigova, N. M. Hannett, D. S. Day, B. J. Abraham, M. A. Cohen, B. Nabet, D. L. Buckley, Y. E. Guo, D. Hnisz, R. Jaenisch, J. E. Bradner, N. S. Gray, and R. A. Young. 2017. YY1 is a structural regulator of enhancer-promoter loops. Cell 171:1573–1588.

Whyte, W. A., D. A. Orlando, D. Hnisz, B. J. Abraham, C. Y. Lin, M. H. Kagey, P. B. Rahl, T. I. Lee, and R. A. Young. 2013. Master transcription factors and mediator establish super-enhancers at key cell identity genes. Cell 153:307–319.

Wu, T., G. Y. Yu, J. Xiao, C. Yan, H. Kurihara, Y. F. Li, K. F. So, and R. R. He. 2018b. Fostering efficacy and toxicity evaluation of traditional Chinese medicine and natural products: chick embryo as a high throughput model bridging in vitro and in vivo studies. Pharmacol. Res 133:21–34.

Wu, J., Y. Zhao, Y. K. Park, J. Y. Lee, L. Gao, J. Zhao, and L. Wang. 2018a. Loss of PDK4 switches the hepatic NF-κB/TNF pathway from pro-survival to pro-apoptosis. Hepatology 68:1111–1124.

Xu, Y., Y. Zhu, S. Hu, Y. Xu, D. Stroup, X. Pan, F. C. Bawa, S. Chen, R. Gopoju, L. Yin, and Y. Zhang. 2021. Hepatocyte nuclear factor 4α prevents the steatosis-to-NASH progression by regulating p53 and bile acid signaling (in mice). Hepatology 73:2251–2265.

Yánez, D. C., C. I. Lau, E. Papaioannou, M. M. Chawda, J. Rowell, S. Ross, A. Furmanski, and T. Crompton. 2022. The pioneer transcription factor foxa2 modulates T helper differentiation to reduce mouse allergic airway disease. Front. Immunol. 13:890781–890793.

Yang, S., Z. Wei, J. Wu, M. Sun, Y. Ma, and G. Liu. 2021a. Proteomic analysis of liver tissues in chicken embryo at Day 16 and Day 20 reveals antioxidant mechanisms. J. Proteomics. 243:104258–104267.

Yang, T., M. Poenisch, R. Khanal, Q. Hu, Z. Dai, R. Li, G. Song, Q. Yuan, Q. Yao, X. Shen, R. Taubert, B. Engel, E. Jaeckel, A. Vogel, C. S. Falk, A. Schambach, D. Gerovska, M. J. Araúzo-Bravo, F. W. R. Vondran, T. Cantz, N. Horscroft, A. Balakrishnan, F. Chevessier, M. Ott, and A. D. Sharma. 2021b. Therapeutic HNF4A mRNA attenuates liver fibrosis in a preclinical model. J. Hepatol. 75:1420–1433.

Zabidi, M. A., and A. Stark. 2016. Regulatory enhancer-core-promoter communication via transcription factors and cofactors. Trends Genet 32:801–814.

Zhao, M., H. Zhao, J. Deng, L. Guo, and B. Wu. 2019. Role of the CLOCK protein in liver detoxification. Br. J. Pharmacol. 176:4639–4652.

Zhao, Y., M. Tran, L. Wang, D. J. Shin, and J. Wu. 2020. PDK4-deficiency reprograms intrahepatic glucose and lipid metabolism to facilitate liver regeneration in mice. Hepatol. Commun. 4:504–517.

Zheng, Y. C., J. Chang, L. C. Wang, H. M. Ren, J. R. Pang, and H. M. Liu. 2019. Lysine demethylase 5B (KDM5B): a potential anti-cancer drug target. Eur. J. Med. Chem. 161:131–140.

Zhu, Y., Q. Zeng, F. Li, H. Fang, Z. Zhou, T. Jiang, C. Yin, Q. Wei, Y. Wang, J. Ruan, and J. Huang. 2020. Dysregulated H3K27 acetylation is implicated in fatty liver hemorrhagic syndrome in chickens. Front. Genet. 11:574167–574182.